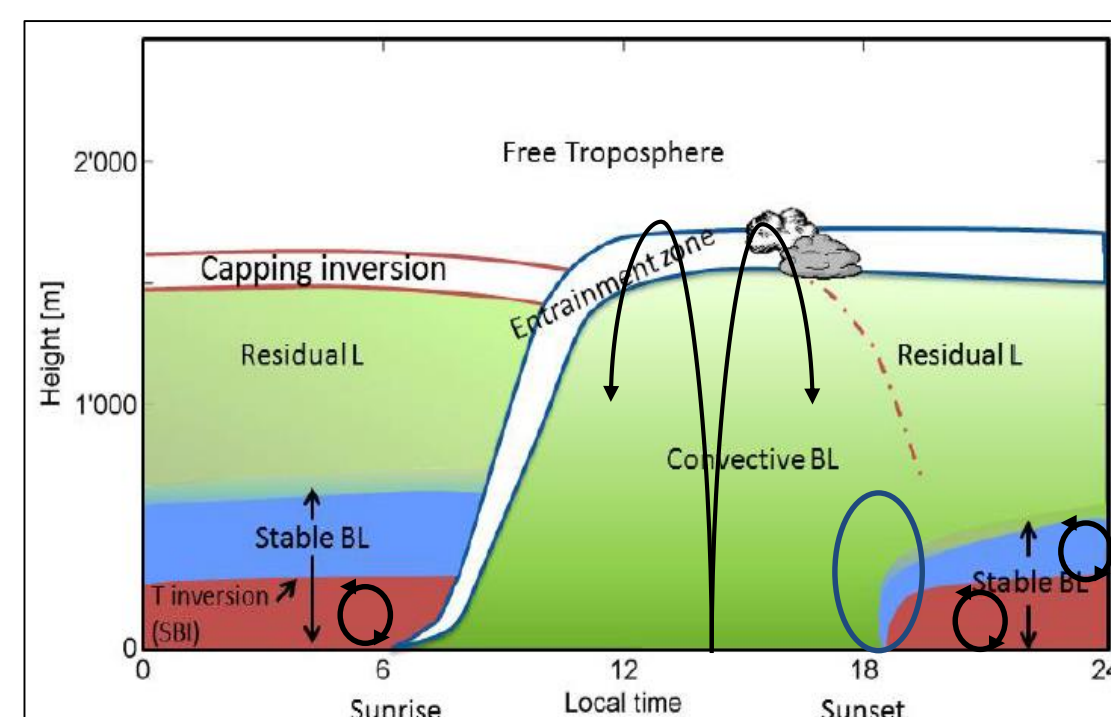


Jon A. Arrillaga <sup>(1)</sup>, Carlos Yagüe <sup>(1)</sup>, Carlos Román-Cascón <sup>(1, 2)</sup>, Mariano Sastre <sup>(1)</sup>, Jordi Vilà-Guerau de Arellano <sup>(3)</sup>, Gregorio Maqueda <sup>(1)</sup>

(1) DEPT. FÍSICA DE LA TIERRA Y ASTROFÍSICA, UNIVERSIDAD COMPLUTENSE DE MADRID, SPAIN ([jonanarr@ucm.es](mailto:jonanarr@ucm.es)) (2) LABORATOIRE D'AÉROLOGIE, UNIVERSITY OF TOULOUSE, CNRS, FRANCE (3) METEOROLOGY AND AIR QUALITY GROUP, WAGENINGEN UNIVERSITY, NETHERLANDS

## 1. MOTIVATION

Over complex-terrain regions a mountain-breeze circulation is formed during fair-weather days. Close to sunset, the cooling of the slopes induces local downslope (hereinafter katabatic) flows. Since their onset takes place during the afternoon and evening transition of the ABL (see Fig. 1), in this work **we pursue gaining knowledge on the complex interaction between the katabatic winds and turbulence** at that stage.



**Figure 1.** Diurnal cycle of the Atmospheric Boundary Layer (ABL) over land on a fair-weather summer day. Adapted from Collaud Coen *et al.* (2014). The blue ellipse indicates the time of the afternoon and evening transition of the ABL.

Understanding that interaction brings relevant information about the nature of the katabatic winds, the formation of surface-based inversions and the associated dew, frost and fogs, pollution diffusion in urban areas, etc.

## 2. OBSERVATIONS

We employ data from *La Herrería Forest*, located at the foothill of the Guadarrama Mountain Range in Spain, at around 40 km from the city of Madrid (Fig. 2).

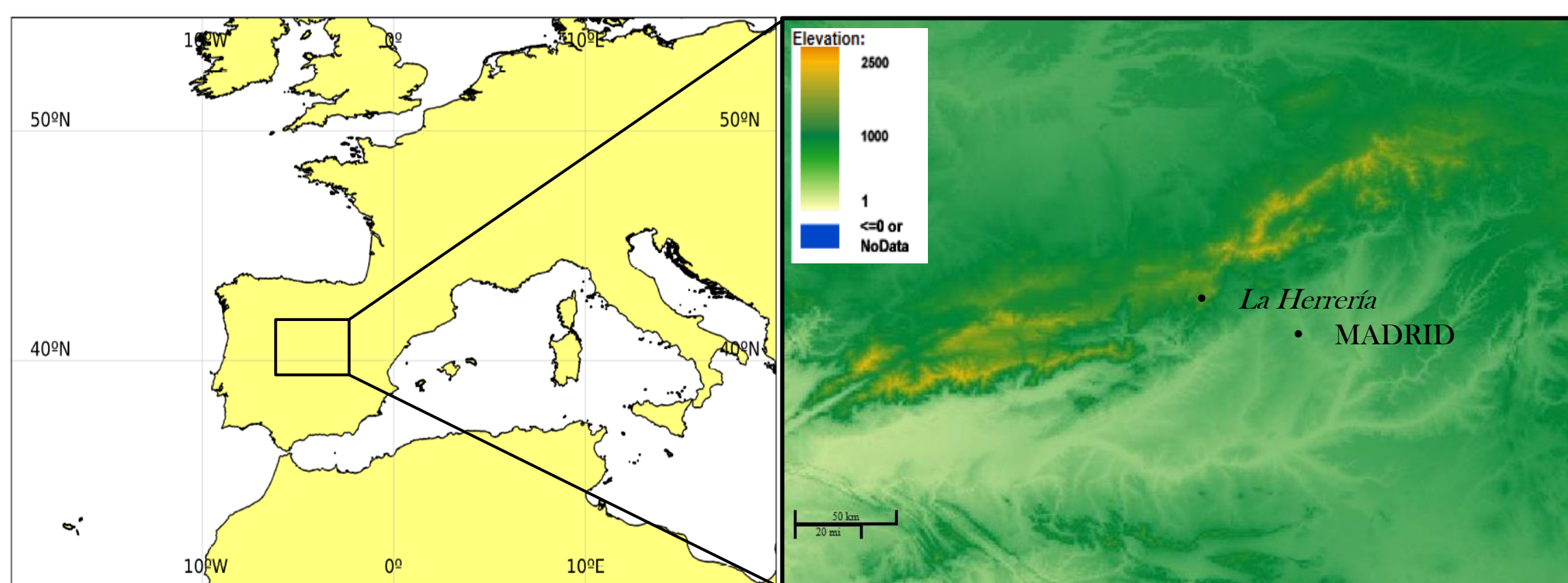


**Figure 2.** Location of *La Herrería* site and the city of Madrid (Spain). The source of topography data is ASTER GDEM (METI, NASA).

This area is characterised for having very dry summers. In this study we use 10-minutal meteorological measurements (see Fig. 3) carried out during an intensive summer campaign in 2017 (22/06 – 26/09).



**Figure 3.** Picture of the 10-m meteorological fixed tower at *La Herrería* Forest during Summer 2017. Wind speed and temperature are measured at 3, 6 and 10 m with cup anemometers and aspirated thermometers respectively, and wind direction at 10 m with a wind vane. CO<sub>2</sub> and water-vapour concentration and turbulent fluxes are measured at 4 and 8 m with IRGASON devices. Besides, precipitation and soil-humidity measurements are also carried out. *La Herrería* is part of the Guadarrama Monitoring Network (**GuMNet**; [www.ucm.es/gumnet/](http://www.ucm.es/gumnet/)).

## 3. SELECTION ALGORITHM

We employ a systematic algorithm (Arrillaga *et al.*, 2018) to select a robust and objective database of katabatic events under **fine-weather conditions**. The selection criteria ensures the following:

- ✓ The **large-scale wind** is weak ( $V_{850} < 6 \text{ m s}^{-1}$ ) and **synoptic cold fronts** are discarded.
- ✓ Days with **convective showers** ( $pp > 0.5 \text{ mm}$ ) are rejected.
- ✓ The wind blows within the **katabatic direction [250° - 340°]** for at least **two hours** in the afternoon-evening.

## 4. WHAT DO WE LEARN ABOUT THE KATABATIC FLOWS?

### DIRECTION & INTENSITY

After applying the selection algorithm 40 katabatic events are selected out of 94 summer days (see wind rose in Fig. 4). Since the katabatics present different intensities (Fig. 5), we classify them according to the maximum wind speed (MWS) at 6 m after their onset: **weak katabatics** ( $MWS < 1.5 \text{ m s}^{-1}$ ) and **intense katabatics** ( $MWS > 3.5 \text{ m s}^{-1}$ ). The weak ones are associated with intense surface thermal inversions and very weak turbulence. On the contrary, the intense ones give rise to important turbulence outbreaks (the TKE and  $u$ , maxima are even greater than the typical diurnal maxima), and surface thermal inversions are broken down.

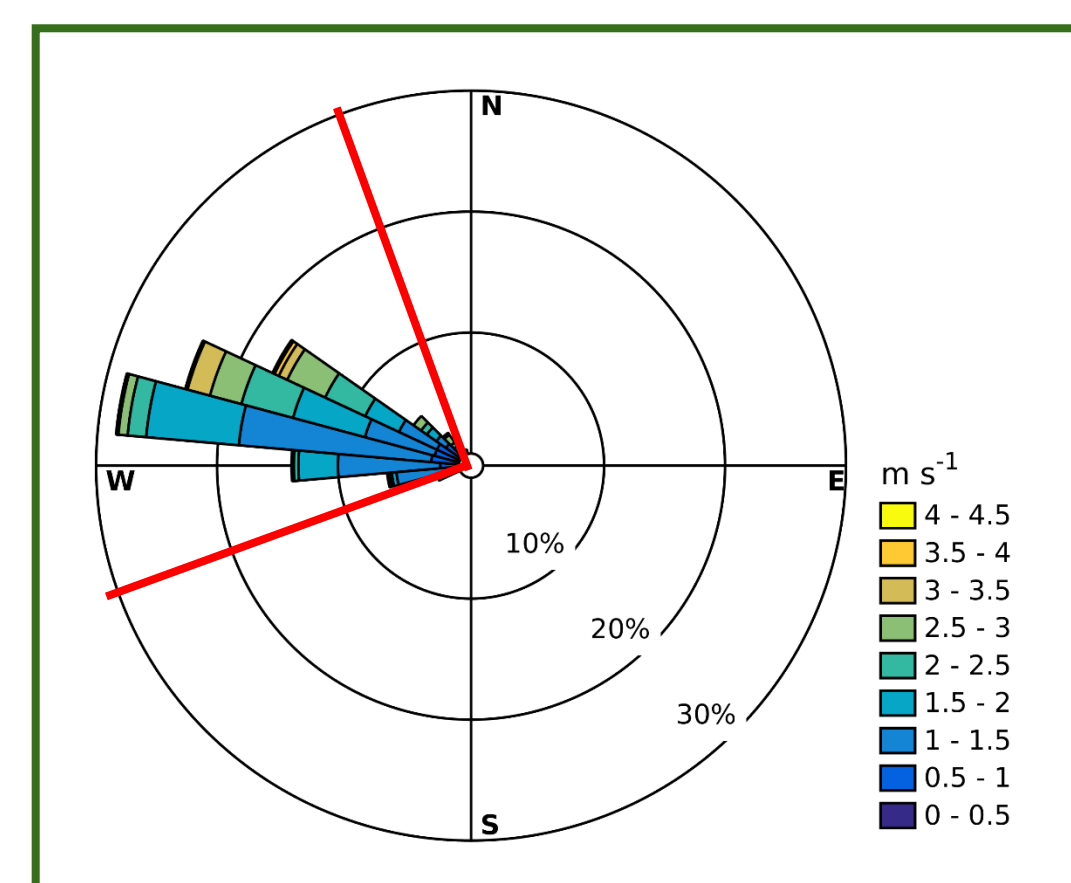


**Figure 4.** Wind rose at 10 m over the 2 h after the onset of the katabatic flow for the 40 selected events.

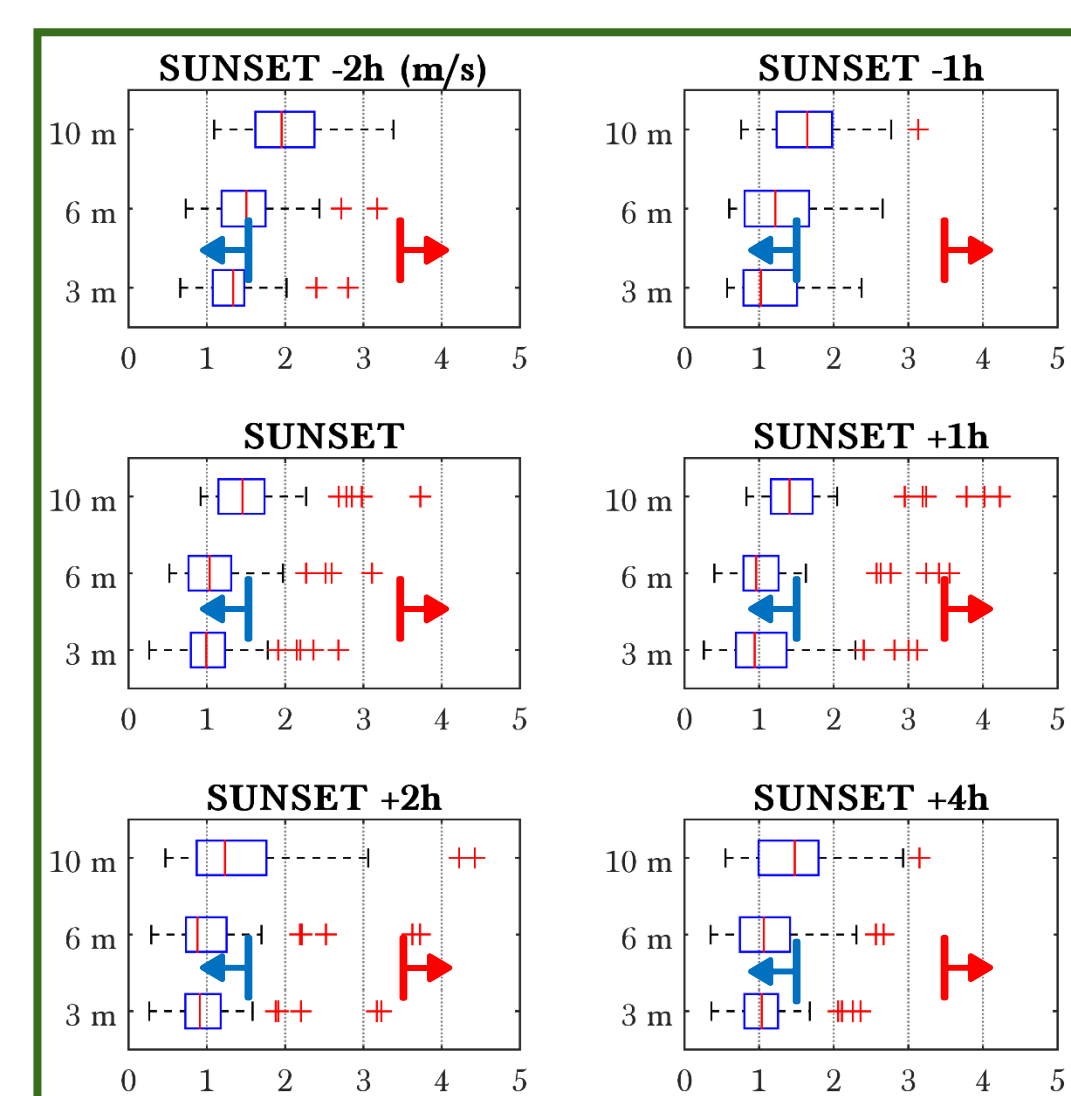


**Figure 5.** Boxplots of the wind speed ( $\text{m s}^{-1}$ ) at 3, 6 and 10 m for the katabatic events, at different times with respect to sunset. The red vertical line within the blue box represents the median, the blue box delimits the first and third quartiles ( $q_1$  and  $q_3$  respectively), the whiskers delimit the most extreme points not considered outliers, and the outliers (red crosses) are drawn if they are greater than  $q_3 + 1.5(q_3 - q_1)$  or smaller than  $q_1 - 1.5(q_3 - q_1)$ . The blue and red arrows indicate the wind-speed thresholds for weak and intense katabatics respectively.

### ORIGIN

We analyse the origin of katabatics of different intensities by exploring the role of the **synoptic wind**, **soil moisture** and **temperature inversion** at the time of the onset. Intense katabatics occur when the large-scale wind blows from the N-NW (Fig. 6), i.e. perpendicular to the mountain range (see Fig. 2), independently of its intensity, and they also form under low soil moistures and surface temperature inversions not yet formed (Fig. 7). On the contrary, weak katabatics establish particularly under W-SW and S-SE large-scale winds. Besides, the surface-based inversion is almost always already formed at their onset and the increase of their intensity is limited by the strong stratification of the stable boundary layer (SBL). We therefore explore the challenging interaction between katabatics and turbulence.

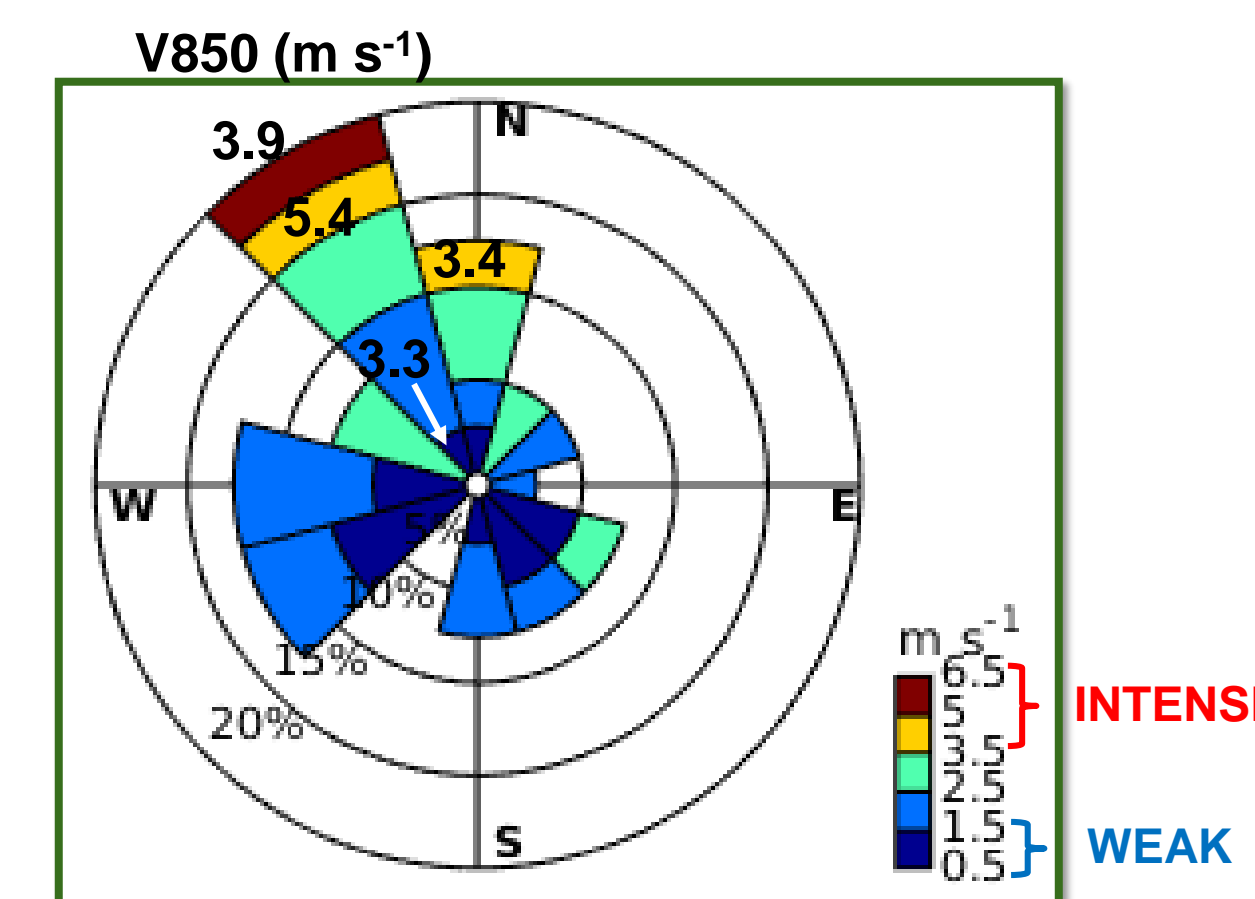


**Figure 6.** Wind rose representing the large-scale wind direction at 850 hPa from NCEP reanalysis at the closest grid point to *La Herrería* (40.5° N, 4° W), together with the observed maximum katabatic wind speed at 6 m. The reanalysis wind speed at 850 hPa ( $V_{850}$ ) for some N-NW events is pinpointed in the wind rose. The colour-ranges corresponding to the weak and intense katabatics are indicated in the scale.

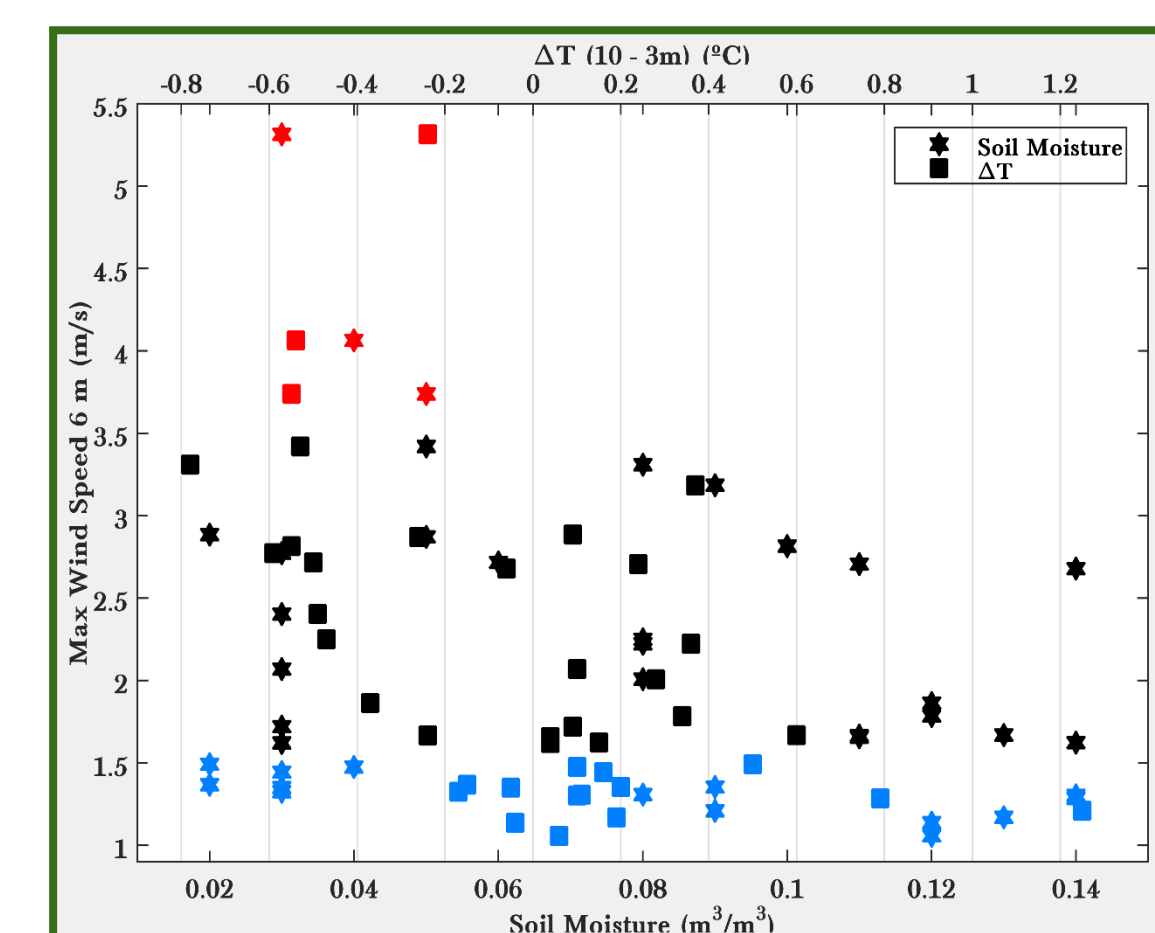


**Figure 7.** Maximum wind speed at 6 m for each katabatic event versus soil moisture at 4-cm depth and the temperature difference between 10 and 3 m. Soil moisture is represented with stars and the temperature differential with squares, in blue for weak, in red for intense and in black for the rest of katabatics.

### INTERACTION WITH TURBULENCE

We find a two-way relationship between the intensity of katabatics and turbulence. In some events where the surface inversion is not yet formed at the onset of the katabatic flow, their intensity increases progressively reaching a weakly-stable regime (a weak inversion is formed). Then, the increase of the wind speed induces an increase of mechanical turbulence and subsequently of the downward heat flux, eroding the surface inversion. Hence, **the interaction between katabatics and turbulence is driven by positive feedbacks**. The different types of katabatics are directly associated with different SBL regimes (Fig. 8). We find that the HOST transition occurs for a smaller  $V_z$  ( $z = 6 \text{ m}$ ) than in *Sun et al.* (2012):  $1.5 \text{ m s}^{-1}$  vs  $2.5 \text{ m s}^{-1}$ . Over complex terrain the advection caused by katabatics favours the generation of bulk shear within regime 2. In fact, that advection is responsible for the non-existence of a clear SBL regime-transition when representing  $\Delta T$  vs shear capacity (SC) (Fig. 9), which was observed in *Van Hooijdonk et al.* (2015) over flat and homogeneous terrain. Furthermore, the relationship between both is dependent on  $z$ , unlike in *Van Hooijdonk et al.* (2015).

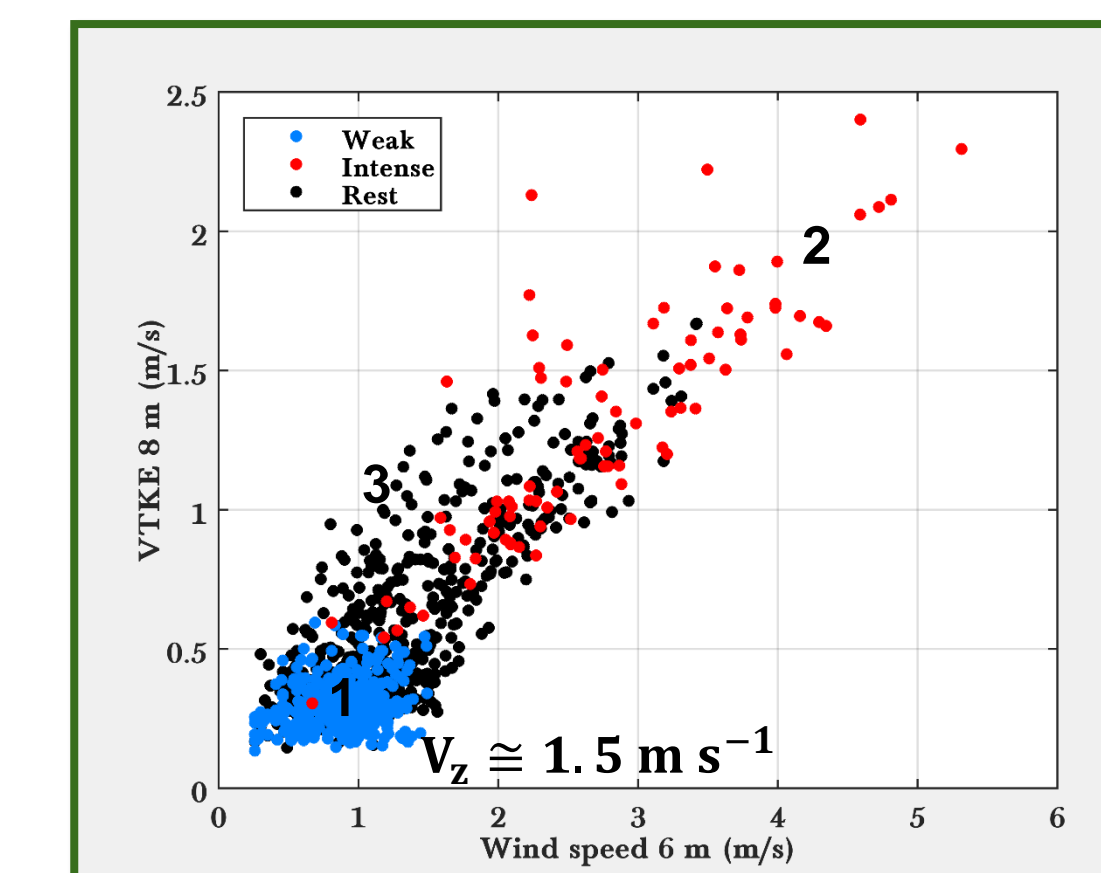


**Figure 8.** Turbulent velocity scale ( $VTKE = \left( \frac{1}{2} (\overline{u'^2} + \overline{v'^2} + \overline{w'^2}) \right)^{1/2}$ ) at 8 m with respect to the wind speed at 6 m, in coloured dots for the katabatics of different intensities. The numbers pinpoint the SBL regimes defined in *Sun et al.* (2012): (1) weak turbulence driven by local instabilities, (2) intense turbulence driven by the bulk shear, and (3) moderate turbulence driven by top-down events. The threshold wind-speed ( $V_z$ ) at which the HOST transition occurs is indicated too.

$$SC = \frac{\partial u}{\partial z} \bigg|_{min} = \left( \frac{(kz)^2 \left( \frac{\partial u}{\partial z}(z) \right)^3}{\theta_1 \theta_0' w' \theta_0'} \right)^{1/3} \quad (1)$$

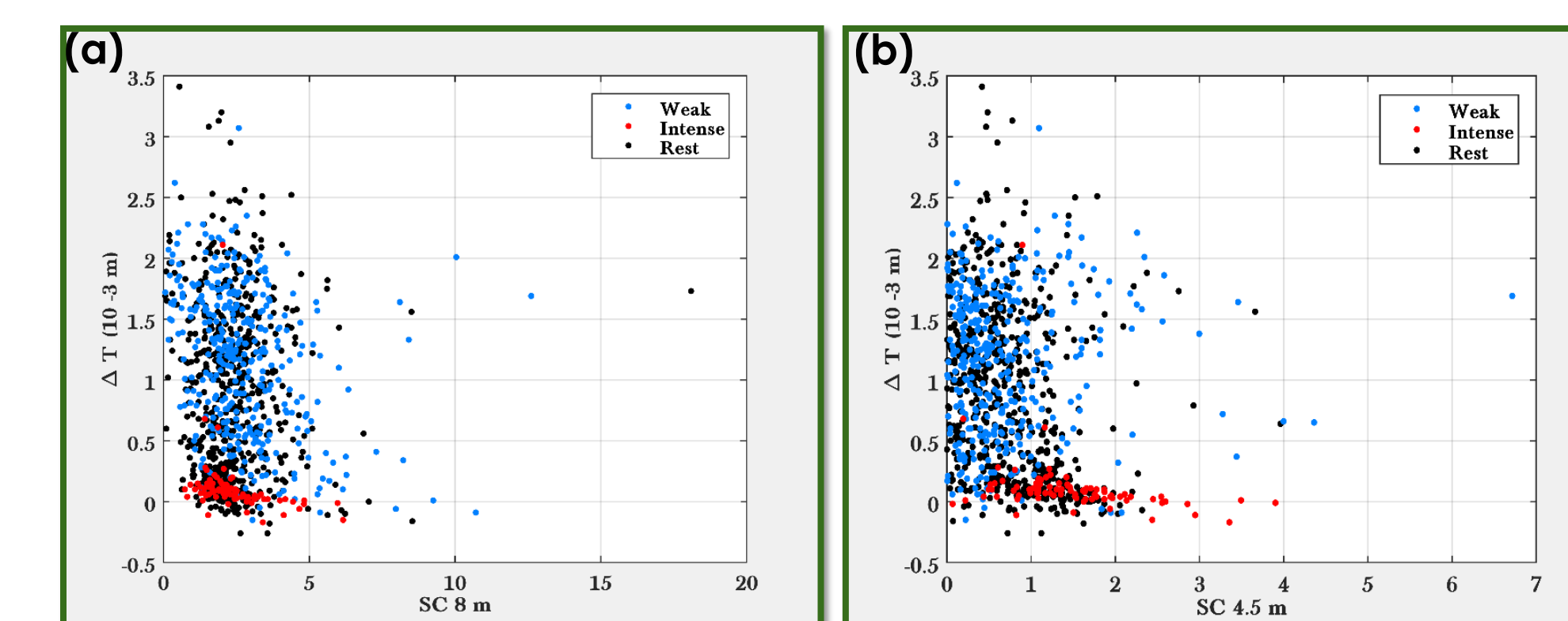


**Figure 9.** Surface temperature inversion versus the shear capacity (calculated using Eq. 1) at 8 m (a) and 4.5 m (b), in coloured dots for katabatics of different intensities.

## 5. TAKE-HOME MESSAGES

- Weak katabatics are associated with strongly stable ABL regimes and intense katabatics, however, with weakly stable regimes.
- Intense katabatics are modulated by the direction of the synoptic wind, soil moisture and the stratification at the onset time. For weak katabatics, the relationship is unclear.
- The interaction between katabatic flows and turbulence is bidirectional and driven by positive feedbacks.
- Over complex terrain the advection term gains importance, and the regime transition in the SBL needs to be characterised differently than over flat terrain.

## 6. REFERENCES

- Arrillaga, J.A., Vilà-Guerau de Arellano, J., Bosveld, F., Baltink, H.K., Yagüe C., Sastre, M., and C. Román-Cascón, 2018: Impacts of afternoon and evening sea-breeze fronts on local turbulence, and CO<sub>2</sub> and radon-222 transport. *Q. J. R. Meteorol. Soc.*, **doi: 10.1002/qj.3252**.
- Collaud Coen, M., Praz, C., Haeefele, A., D. Ruffieux, D., Kaufmann, P. and B. Calpini, 2014: Determination and climatology of the planetary boundary layer height above the Swiss plateau by in situ and remote sensing measurements as well as by the COSMO-2 model. *Atmos. Chem. Phys.*, **14**, 13205–13221.
- Sun, J., Mahrt, L., Banta, R.M. and Y.L. Pichugina, 2012: Turbulence regimes and Turbulence Interimmetry in the stable boundary layer during CASES-99. *J. Atmos. Sci.*, **69**, 338–351.
- van Hooijdonk, I.G.S., Donada, J.M.M., Clerex, H.J.H., Bosveld, F.C., and B.J.H. van de Wiel, 2015: Shear capacity as prognostic for nocturnal boundary layer regimes. *J. Atmos. Sci.*, **72**, 1518–1532.

## 7. ACKNOWLEDGEMENTS

This research has been funded by the ATMOUNT-II project [Ref. CGL2015-65627-C3-3R (MINECO/FEDER)] and the Project [Ref. CGL2016-81828-REDT/AEI] from the Spanish Government, and by the GuMNet [Guadarrama Monitoring Network, [www.ucm.es/gumnet/](http://www.ucm.es/gumnet/)] observational network of the CEI Moncloa campus of International Excellence. Jon A. Arrillaga is supported by the Predoctoral Training Program for No-Doctor Researchers of the Department of Education, Language Policy and Culture of the Basque Government (PRE\_2017\_2\_0069, MOD = B). We thank the contribution of all the members of the GuMNet Team.